SURFACE ROUGHNESS EFFECT ON UNDERWATER DYNAMIC NOISE ENERGY TRANSPORT

V. Shchurov Pacific Oceanological Institute FEB RAS
V. Kouleshov 43, Baltiyskaya Str., Vladivostok, Russia, 690041
M. Kuyanova E-mail: shchurov@poi.dvo.ru

1. INTRODUCTION

Directional properties of underwater ambient dynamic noise in the 400-700 Hz frequency band have studied. Arrangement in the dynamic noise energy flux density vector has been used as an indicator of the noise energy transport direction in deep water. A series of experimental trials has been done at various near-surface wind speeds (6 to 12 m/s) and various intensities of the surface roughness. It was that the dynamic noise energy flux density vector possesses both vertical and horizontal components. The horizontal component forming mechanism involves the initial noise field scattering on the rough surface. Statistical properties of the surface roughness one can estimate using statistical properties of the vertical and horizontal components of the energy flux density vector.

2. VECTOR PROPERTIES OF UNDERWATER AMBIENT NOISE IN THE 6-800 HZ FREQUENCY BAND

Ambient noise measurements have been made in 6-800 Hz frequency band in deep ocean. The ambient noise energy flux density vector **I**(f,φ,θ) has been estimated in the frequency range of interest (f is the frequency, φ is the azimuth measured from the x-axis, θ is the elevation angle measured from the z-axis). X- and y-axes are in the horizontal plane, z-axis points downward. The direction of vector **I**(f,φ,θ) at every point in space was considered as an indicator of the noise and signal energy transport direction within the ocean waveguide.

Instant values of the azimuth φ and the elevation angle θ of the energy flux density (intensity) vector **I**(f,φ,θ) were calculated in the frequency band Δf_0 at various times of exponent averaging T_0 as follows:

$$\varphi(\Delta f_0, t) = arctn\frac{\mathrm{Re}\, I_y(\Delta f_0, t)}{\mathrm{Re}\, I_x(\Delta f_0, t)} \qquad (1)$$

$$\theta(\Delta f_0, t) = arctn\frac{\left[\mathrm{Re}^2\, I_x(\Delta f_0, t) + \mathrm{Re}^2\, I_y(\Delta f_0, t)\right]^{1/2}}{\mathrm{Re}\, I_z(\Delta f_0, t)} \qquad (2)$$

$I_x(\Delta f_0,t)$, $I_y(\Delta f_0,t)$, $I_z(\Delta f_0,t)$, were calculated from corresponding instant cross spectra $S_{PVx}(\Delta f_0,t)$, $S_{PVy}(\Delta f_0,t)$, $S_{PVz}(\Delta f_0,t)$ (exponent averaging, 4-Hz band of analysis). Eqs. 1 and 2 were used to compute instant spectra φ(f) and θ(f) from $\mathrm{Re}I_x(\Delta f_0,t)$, $\mathrm{Re}I_y(\Delta f_0,t)$, $\mathrm{Re}I_z(\Delta f_0,t)$. Average time used in computing spectra φ(f) and θ(f), was taken to be equal to that average time which provides the least constant standard deviation of the cross-spectra. In Fig. 1 average time is 60 sec. It should be noted that φ(f) and θ(f) remain practically the same while average time is increased until 120 sec.

Fig.1 shows the most typical spectra φ(f) and θ(f) which determine **I**(f,φ,θ) direction in deep ocean over 6 to 800 Hz frequency band. Averaging was done over 60 sec. Fig. 1 evidences that direction of the ambient noise energy transport depends on frequency.

Guided by Fig.1 one can separate 6 to 800 Hz band into three intervals as follows:

Surface roughness effect on underwater dynamic noise energy transport – V. Shchurov, V.Kouleshov, M. Kuyanova

Δf_1=6-20 Hz. Downward directed noise energy flux makes angles 50° to 60° with the z-axis, the azimuth φ is about -120° (see interval AB in Fig. 1). Noise sources contributing to this frequency band are as follows, seismic events, turbulent processes within the ocean/atmosphere boundary layer and manmade sounds.

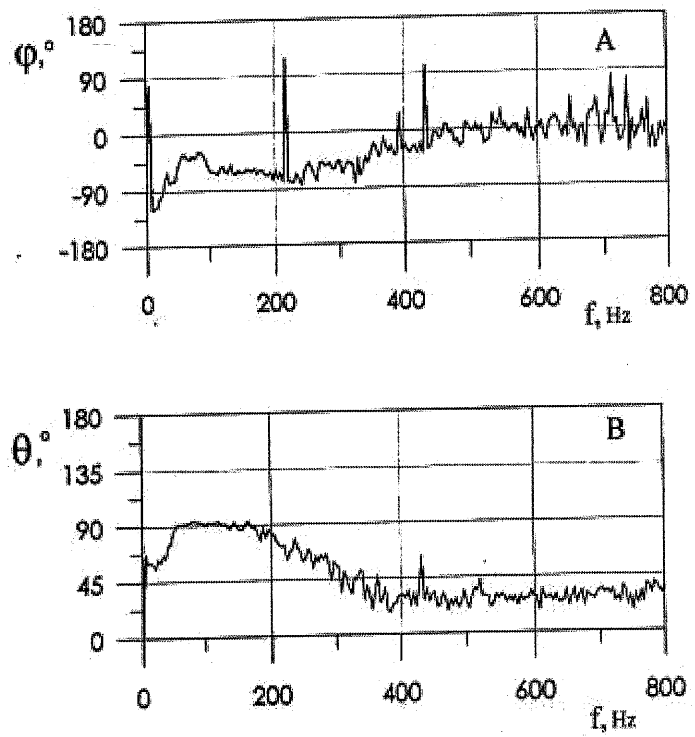

Fig. 1. Spectra of azimuth and elevation angle $\varphi(f)$, $\theta(f)$ of the energy flux density vector of the ambient noise and signals f_1=215 Hz, f_2=430 Hz (deep ocean, depth of the measurement point is 500 m, near-surface wind speed is 6 m/sec). Combined sensor x-axis coincides with the wind speed, z-axis is directed downward. 4-Hz band of analysis, average time is 60 sec.

Δf_2=50-200 Hz. Distant shipping noise prevails. Noise energy flux propagates in the horizontal plane ($\theta(f)\approx 90°$) with azimuths -(45°÷60°) (see interval CD in Fig.1).
There is a transition band 200 to 400 Hz in which shipping-generated noise energy fluxes compete with that of dynamic origin. Dynamic noise becomes dominant above 400 Hz. Signals at 215 Hz and 430 Hz are generated by the research vessel machinery (the combined sensor y-axis is directed toward the research vessel). Azimuths of those signals correspond to the y-axis, $\varphi\approx 90°$ (Fig. 1A).
Δf_3=400-800 Hz. Dynamic noise prevails (see interval EK in Fig. 1). All over the 400 to 800 Hz frequency band $I(f,\varphi,\theta)$ makes an angle about 30° with z-axis, and dynamic noise energy flux density vector $\mathbf{I}(f,\varphi,\theta)$ possesses both vertical and horizontal components. The azimuth $\varphi(f)$ fluctuates about zero. The combined sensor x-axis coincides with the near-surface wind. Hence, to a first approximation horizontal component of the dynamic noise energy flux is aligned with the near-surface wind. As seen from experiments described in Refs.[1-5] the dynamic noise energy

transport in the horizontal plane is more tightly bounded to the surface waves propagation rather than to near-surface wind direction.

3. STATISTICAL CHARACTERISTICS OF VERTICAL AND HORIZONTAL COMPONENTS OF THE DYNAMIC NOISE ENERGY FLUX

Processing of the data collected in deep ocean was done as follows. The frequency range of interest, 400 to 700 Hz was divided into 6 frequency bands the following way: Δf_1=400-450 Hz, Δf_2=450-500 Hz, Δf_3=500-550 Hz, Δf_4=550-600 Hz, Δf_5=600-650 Hz, Δf_6=650-700 Hz. Instantaneous values of $\varphi_i(\Delta f_i,t)$ and $\theta_i(\Delta f_i,t)$ were computed from Eqs. (1) and (2) in a sequence of 4-Hz intervals for each frequency band i=1-6. Then corresponding probability density functions (pdfs) were built and mean values $<\varphi_i>$, $<\theta_i>$ as well as standard deviations $\sigma(\varphi_i)$, $\sigma(\theta_i)$ estimated.

Figs.2 and 3 show 5 pdfs. Curve 1 corresponds to averaging over 1sec, curve 2 – to 3sec average time, 3 – to 5sec, 4 – to 10sec, 5 – to 60sec; frequency bands are: Δf_1=400-450Hz, Δf_6=650-700Hz.

Fig2.The probability density function $\rho(\varphi)$ dependence on average time T_0. Frequency resolution is 4 Hz. Collection time is 300s. The curve **1** corresponds to T_0=1s, the curve **2** to T_0=3s, **3** to 5s, **4** to 10s, **5** to 60 s. Frequency bands: A. 400~450 Hz, B. 650~700Hz.

As seen in Fig.2, when increasing average time, the maximum of φ_i pdf becames more sharp and corresponding $\varphi_{i\ max}$ tends to a certain limit.

Fig.3 illustrates θ_i pdfs (i=1-6) dependence on average time. Figs.2 and 3 correspond to the same interval of the data recording 1800sec long. As seen in Fig.3, $\theta_{i\ max}$ corresponding to the maximum of θ_i pdf tends to its certain limit (individual for each frequency band Δf_i) likewise $\varphi_{i\ max}$ (Fig.2).

Fig.4 shows $<\varphi_i>$ and $<\theta_i>$ for 6 frequency bands Δf_i (i=1-6) and average times T_0=1,3,5,10,20,30,60sec. Mean values $<\varphi_i>$ and $<\theta_i>$ are derived from the corresponding pdfs. Fig.4 evidences that $<\varphi_i>$ and $<\theta_i>$ tend to their certain limits φ_i and θ_i as average time increases. Solid curves in Fig.4 represent theoretical approximations for $<\varphi_i>$ and $<\theta_i>$. From Fig.4 may be inferred that in the horizontal plane for each

frequency band Δf_i (i=1-6) corresponding noise energy flux does not propagate in the same direction as wind. Recall, that x-axis (φ=0°) is aligned with the wind speed vector. At average time T_0=60sec noise energy fluxes related to 550 to 700Hz frequency band (i=4,5,6; $\lambda \approx 2{,}1-2{,}7$m) are most close to the wind direction $<\varphi_{4,5,6}> \approx -5°$. From the other hand, directions of noise energy fluxes related to the lower frequencies 400-550Hz (i=1,2,3; $\lambda \approx 3{,}0-3{,}7$m) more significantly differ from the wind direction: $<\varphi_1> \approx -27°$, $<\varphi_2> \approx -21°$, $<\varphi_3> \approx -13°$.

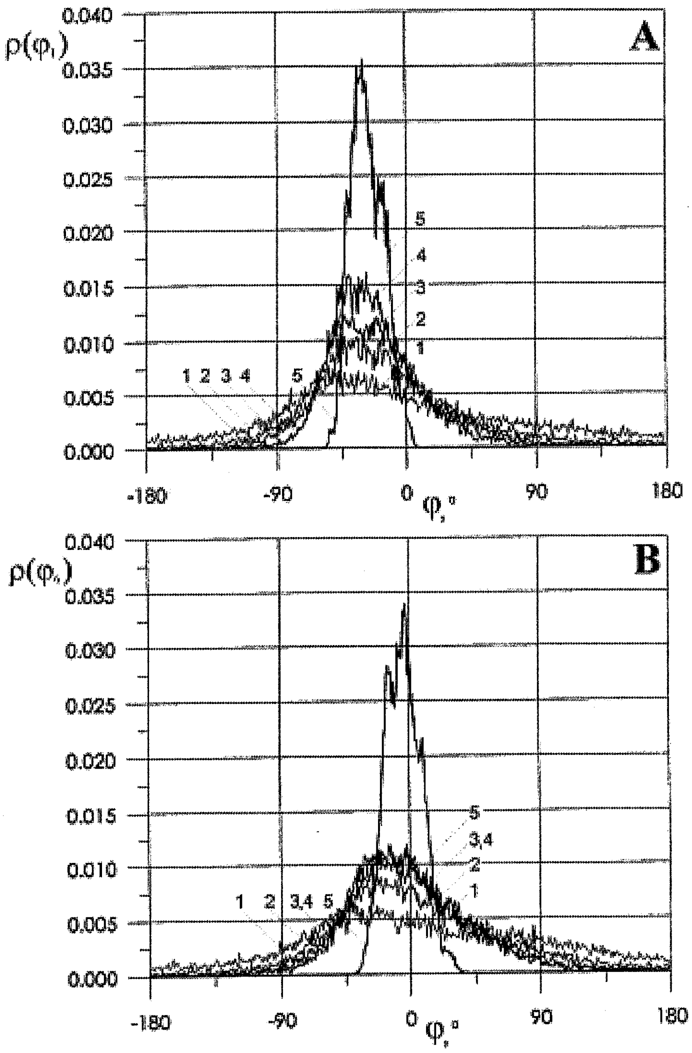
A
ρ(φ1)
0.040
0.035
0.030
0.025
0.020
0.015
0.010
0.005
0.000
1 2 3 4
5
5
4
3
2
1
-180
-90
0
φ,°
90
180
B
ρ(φ2)
0.040
0.035
0.030
0.025
0.020
0.015
0.010
0.005
0.000
1 2 3,4 5
5
3,4
2
1
-180
-90
0
φ,°
90
180

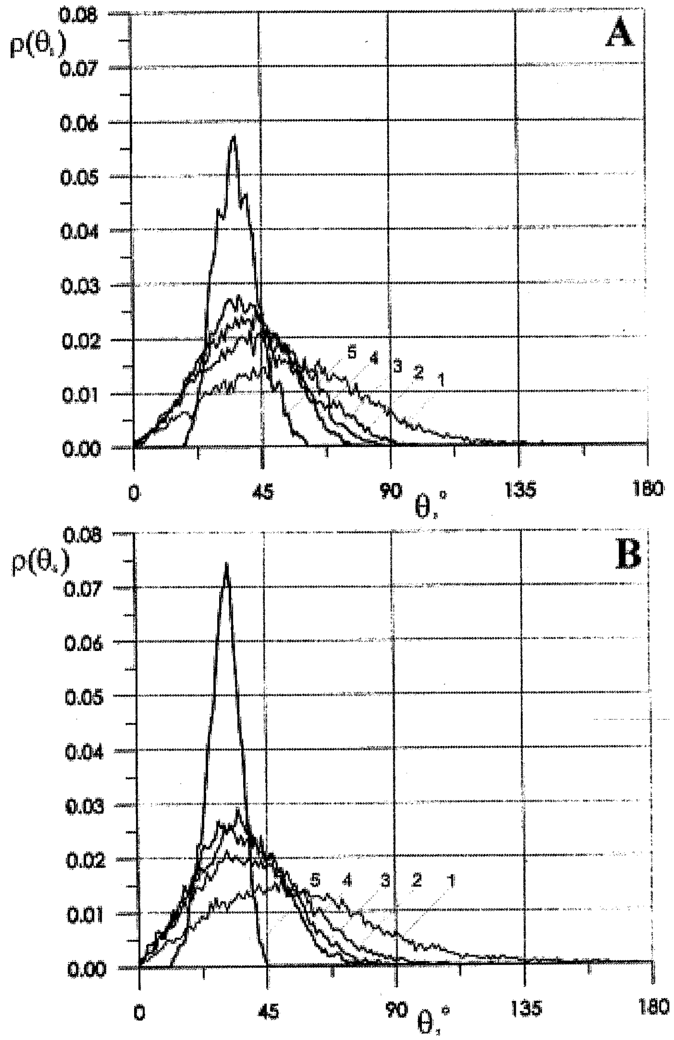

Fig.3 The probability density function $\rho(\theta)$ dependence on average time T_0. Frequency resolution is 4Hz. Collection time is 300s. The curve **1** corresponds to T_0=1s, the curve **2** to T_0=3s, **3** to 5s, **4** to 10s, **5** to 60 s. Frequency bands A 400~450 Hz, B 650~700Hz

Hence, if may be concluded, that the dynamic noise energy transport is frequency dependent in the horizontal plane as well as in the vertical. Note, that the azimuth φ_i and the polar angle θ_i of the noise energy fluxes related to all frequency bands tend to their certain limits $<\varphi_i>$ and $<\theta_i>$ as average time increases from 1sec up to 60sec.
Surface roughness effect on underwater dynamic noise energy transport – V. Shchurov, V.Kouleshov, M. Kuyanova

Fig.4 A. Dynamic noise energy flux azimuth φ dependence on average time. The measurement point dpth is 500 m, wind speed is 6 m/s. B. Dynamic noise energy flux polar angle θ dependence on average time T_0. The measurement point dpth is 500 m, wind speed is 6m/s.

Horizontal dynamic noise energy flux which propagation is correlated with the surface wind waves propagation has been first found in experiments focused on vector characteristics of the

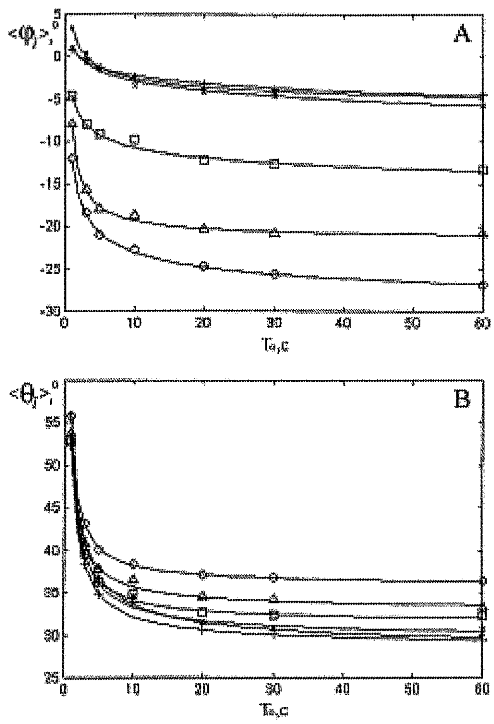

ambient noise field [1].
The correlation revealed among the surface wind waves propagation and that of the horizontal dynamic noise energy flux evidences that anisotropy in the surface waves causes anisotropy in the noise field [6].

Fig.5 The standard deviation σ_{φ} dependence on average time T_0 in different frequency bands. The measurement point depth is 500 m, the wind speed is 6 m/s. The approximation σ_{φ}= a/sqrt(t*c).

Fig.5. shows standard deviation σ_{φ} dependence on average time T_0 for frequency bands Δf_i (i=1-6). Experimental measurements corresponding to T_0=1,30, 60sec were used to compose σ(φ) approximation. Experimental mark corresponding to T_0=20sec agrees with approximation curve whereas marks related to T_0=3,5,10sec lie above the curve. As seen from Fig.5, when averaging over T_0=1sec, σ(φ)≈80° for all frequency bands Δf_i, i.e. in the horizontal plane noise energy is transporting within spatial sector $\Delta\varphi_i$=<φ_i>±80°. In this case the angular value of the sector is about 160°, at T_0=60sec it narrows down to about 20°.

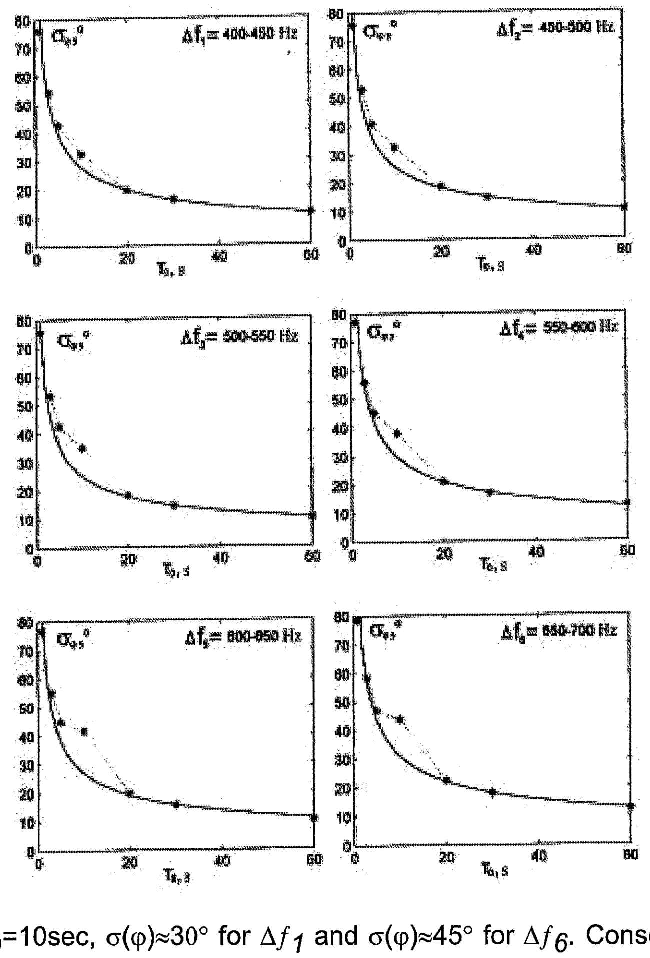

Surface roughness effect on underwater dynamic noise energy transport – V. Shchurov, V.Kouleshov, M. Kuyanova

Fig.6 The standard deviation σ_{θ} dependence on average time T_0 in different frequency bands. The measurement point depth is 500 m, the wind speed is 6 m/s. The approximation $\sigma_{\theta}=a+b/(t^c)$.

Analyzing the dynamic noise over the 400-700Hz frequency band, one may see rise in σ(φ) at T_0=3,5,10sec as the noise frequency increase, e.g. at T_0=10sec, σ(φ)≈30° for Δf_1 and σ(φ)≈45° for Δf_6. Consequently, angular value of the sector in which the dynamic noise energy transports, depends on its frequency. As for σ(θ), it does not behave this way.

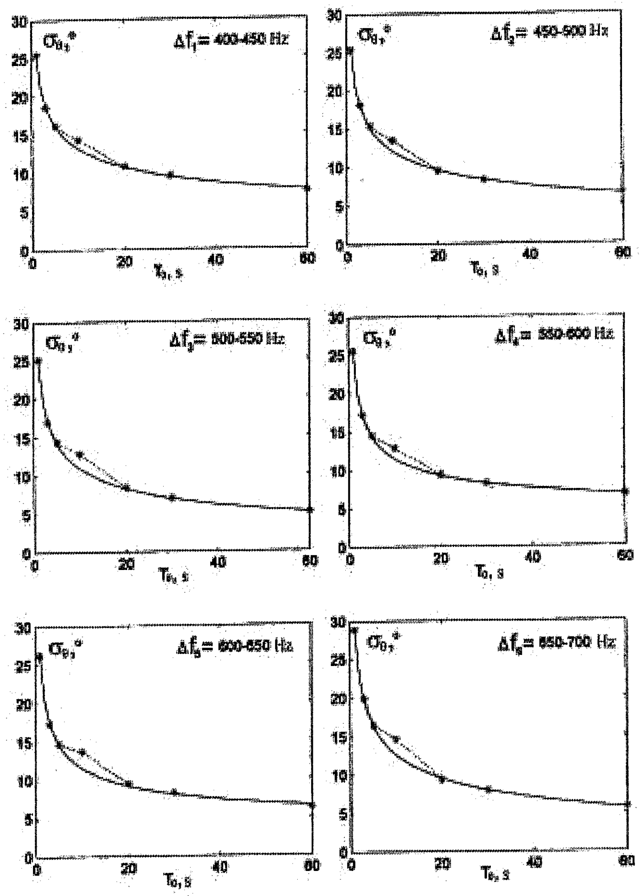

Standard deviation $\sigma(\theta)$ depends on average time T_0 the same way $\sigma(\varphi)$ does (see Figs.5 and 6). The data related to T_0=1,30,60sec were used to built an approximation for $\sigma(\theta)$. Just only one experimental mark (T_0=10sec) does not agree with the approximation curve. At T_0=1sec, $\sigma(\theta)\approx 25°–30°$, i.e. $\Delta\theta_i=<\theta_i>\pm 30°$. At T_0=60sec, $\Delta\theta_i=<\theta_i>\pm 7°$. It is evident, in the vertical plane the angular value of the sector is 60° (at T_0=10sec) or 14° (at T_0=60sec).

4. REFERENCE

1. Shchurov V.A. Coherent and diffusive fields of underwater acoustic ambient noise// J.Acoust.Soc. Am. 1991. V. 90(2). P. 991-1001.
2. Shchurov V.A. Ambient noise energy motion in the near-surface octan layer// Recent Advances in Underwater Acoustics, Proc.I.O.A. 1991.V. 13(3), Weymouth, UK. P. 250-256.
3. Shchurov V.A., Ilyichev V.I., Khvorostov Y.A. Ambient noise anisotropy in horizontal plane// Proc. ICA-14, E1-10. Beijing, China, 1992.
4. Shchurov V.A. et al. The ambient noise energy motion in the near-surface in ocean wake-guide// J. de Physique IV, colloque C5, supplement au Journal de Physique III. France. 1994. V. 4. P. C5, 273-1276.
5. Shchurov V.A. et al. A possidle mechanism of dynamic ambirnt ocean noise horizontal energy flow forming// Proc. I.O.A. Arrays and Beamforming in Sonar. University of Bristol. UK. 1996. P. 121-127.
6. Shchurov V.A. et all. Vector acoustics of the ocean. Chapter V. Vladivostok. Dalnauka. 2000. 60 p.